Chapter 4

Computational study of the structural and dynamic insights of membrane bound α-Synuclein at atomistic level resolution

Computational study of the structural and dynamic insights of membrane bound α-Synuclein at atomistic level resolution

4.1. Abstract:

PD has been associated with α-Syn, a presynaptic protein that attaches to cell membranes. The molecular pathogenesis of PD most likely begins with α-Syn binding to membranes. The α-Syn molecule may assume several shapes. In water, it is mostly amorphous, but when it is attached to lipid bilayers and similar membrane-like surfaces, it can take on a variety of dynamic conformations. Using all-atom MD simulation study, we have carried out the study to determine the conformational stability of α-Syn in membrane bound state. The MD trajectories were used to analyze the structural flexibility and stability of α-Syn as a function of simulation time. The conformational snapshots of α-Syn showed that the amount of α-helices in the secondary structure of α-Syn decreases as simulation time progresses. Also, the free energy profile of α-Syn suggested the energy difference between global minima and secondary minima. The percentage of probable secondary structure were calculated to be 18.9% using YASARA software. The hydrogen bond analysis of inter-molecular between membrane bilayer and α-Syn was studied to determine the proximity of protein during the simulation time period. This study has thus helped us to understand that α-Syn protein in membrane bound state affects structural and conformational properties of the protein.

4.2. Introduction:

PD has been associated with α-Syn, a presynaptic protein that attaches to cell membranes. The molecular pathogenesis of PD most likely begins with α-Syn binding to membranes. The α-Syn molecule exhibits several conformations: it is mainly disordered in water, assumes a β-sheet conformation in amyloid fibrils, and forms a dynamic multiplicity of α-helical conformations when it is coupled to lipid bilayers and comparable membrane-mimetic surfaces. A protein called α-Syn has been linked to neurodegenerative conditions such as PD and LB dementia [307]. Since it has been demonstrated to be necessary for SNARE complex formation at the presynaptic membrane, α-Syn's lipid bilayer association is believed to be significant for its biological role in controlling synaptic vesicles [131, 308]. It is believed that misfolded or aggregated α-Syn interacts with the lipid bilayer part of cell membranes to cause toxicity to neurons. The potential pathways of interaction between α-Syn and lipid bilayers is determined therefore crucial to comprehending α-Syn's mechanism of action and, eventually, to open up new avenues for pharmacological development targeted at mitigating or reversing

its effects on cells [309, 310]. However, several following studies [311-313] suggested that an equilibrium may exist between populations of extended and broken helices, and that the broken helix conformation may adopted by α-Syn attached to the membrane. Furthermore, it should be mentioned that the disordered C-terminal tail of α-Syn contains 10 glutamate and 5 aspartate residues, so it is unlikely to form favorable interactions with an anionic lipid bilayer. The α-helical N-terminal segment of α-Syn contains seven KTKEGV motifs, which are thought to play a role in maintaining an unfolded state in solution [314]. Overall, it would appear that, depending on the membrane's composition and curvature, the N-terminal region of α-Syn may adopt an extended or dynamically disturbed α-helical conformation when coupled to a surface [315]. After attaching to a membrane, α-Syn folds differently, taking on an α-helical shape across the course of its 60 N-terminal residues [19, 165]. Imperfect sequence repeats of 11 residues, which can fold into amphipathic α-helices and bind lipid membranes by laying parallel at the interface between the polar lipid heads and the hydrophobic interior of the membrane, facilitate this ordering process [316-318]. In order to better understand the conformational dynamics of α-Syn and related proteins in aqueous solution [227, 319-322] and when attached to membranes, computational methods in particular molecular docking have been crucial. Furthermore, it has been demonstrated that MD simulations [91, 323-328] are an effective method for describing how membrane proteins interact with lipids [329, 330] and other molecular surfaces. The pathophysiological significance of α-Syn can be better understood by comprehending its potential conformations when interacting with a cell membrane model. This is because treatment strategies involving the regulation of membrane binding remain viable [81]. Five distinct helices are predicted by sequence analysis employing apolipoprotein algorithms [331]. In accordance with previous studies, monomeric α-Syn's interaction with negatively charged vesicles results in the formation of a mainly helical shape in the protein's N-terminal region [331]. A "double-anchor" mechanism was defined, wherein the core regions and N-terminal of α-Syn temporarily attach to two distinct vesicles, hence facilitating their indirect contact. According to recent study [332], this process is strengthened when calcium binds to the C-terminal. The capacity of membrane-bound α-Syn to interact with a second vesicle is also dependent on kinetic considerations, as this active conformation is only momentarily filled in the conformational ensemble [18]. In this regard, the current discovery that membrane binding in the area 87–97 is independent of protein conformation suggests a kinetically simpler binding mechanism that obviates the need for a folding-upon-binding phase. The tendency of α-Syn to self-assemble into amyloid fibrils is also strongly influenced by membrane contacts; in some

situations, the presence of lipid vesicles accelerates the aggregation process by many orders of magnitude [333]. Thus, the primary objectives of this work were to devise a methodology for understanding the folding and unfolding of the structure bound to the membrane and to use this methodology to ascertain the three-dimensional structure of membrane-bound α-Syn.

4.3. Materials and Methods:

4.3.1. Preparation of membrane bound α-Synuclein complex structure:

The WT α-Syn was uploaded to initiate the construction of the membrane bilayer using the CHARMM GUI server. The CHARMM general force field is used to read the hetero chain residue, and the initial orientation of the protein with respect to the lipid/water interface was predicted using the PPM server [334]. The negatively charged side chains were oriented away from the membrane, while the lysine side chains were oriented towards the membrane surface. The input files for MD calculations were prepared using the web-based graphical interface CHARMM-GUI [334]. The lipid bilayers were built from phosphatidylethanolamine (PE), phosphatidylcholine (PC), and phosphatidylserine (PS) using the CHARMM-GUI server. This lipid bilayer composition was selected because it excellently mimics the synaptic vesicles [317]. Membrane bilayer consisting of DOPE, DOPS, and DOPC in a ratio of 5:3:2 and model it with lipid17 force field parameters and the similar composition of lipid membrane was employed in our study [25]. Followed by adding 0.15M KCl concentration using the Monte Carlo ion placing method to neutralize the system. Both systems are assembled and use the charmmlipid2amber.x script, the CHARMM-generated file is converted to AMBER format. UCSF Chimera software alpha v.1.12 [220] was used to visualize this complex structure, separate the ligand and receptor, and save their coordinates in mol2 and PDB formats. The Antechamber protocol in xleap curated the chosen solution structure. Bcc charge, frcmod file, and complex systems in explicit and implicit solvation are required. Topology and coordinate files were then created for each system. The explicit solvation was used for complex system MD simulations.

4.3.2. Molecular Dynamics Simulation protocol:

The MD simulation was performed using the AMBER 18 simulation package [335] with the force field ff99SBildn [305]. To solvate the protein, a rectangular box with a minimum distance of 10 Å to the edges of the box was employed. The TIP4PEW water model was used. To neutralize the system, the required number of counter ions was added. The calculations were done at a temperature of 300 K and a pressure of 1 bar. The Particle Mesh Ewald MD

module [205, 227] was employed for the correct treatment of long-range electrostatic interactions. The minimization and equilibration of the system were performed for 100 ps and 1 ns, respectively. The time step for MD simulations was calculated to be 2 fs. The trajectories and coordinates were obtained for further analysis. The topology and coordinate files for WT α-Syn were carried out using the Leap module of the AMBER18 software package. The topology and co-ordinate files were generated. The missing hydrogen atoms and heavy atoms were added using the AMBER force field ff99SBildn. From the literature review, it was observed that the ff99SB force field has been used in many of the studies to characterize the structural features of intrinsically disordered proteins [227, 336-339]. A two-step energy minimization was performed to avoid the steric hindrances. After minimization, the system was gradually heated from 0 to 300 K for a time-period of 100 ns with constraints on the solute and thereby maintained in the isothermal-isobaric ensemble (NPT). The temperature of the system was kept at a target temperature of 300 K and a pressure of 1 atm. MD for constant pressure-temperature conditions (NPT) with temperature regulation was accomplished by employing the Berendsen weak coupling approach (0.5 ps time constant for heat bath coupling and 0.2 ps pressure relaxation time). Subsequently, using the Berendsen weak coupling method [340] (0.5 ps time constant for heat bath coupling and 0.2 ps pressure relaxation time), MD for constant pressure-temperature conditions (NPT) with temperature regulation was achieved. For treating the long-range electrostatic interactions, the PME method was used with the default parameters. For non-bonded interactions, the cut off value was set to 9 Å. After reaching the target temperature, the systems were equilibrated for a time period of 500 ps, and thereby the production run proceeded for 100 ns in the isothermal-isobaric ensemble. A production run was conducted using the Berendsen barostat with a collision frequency and pressure relaxation time of 2 ps and 1 ps, respectively. The Shake algorithm [341] was used to constrain the bonds between hydrogen atoms.

4.3.3. Analysis of Molecular Dynamics Trajectories:

Structural analysis of MD simulation for the α-Syn was performed using the CPPTRAJ module [305, 342, 343] of AmberTools 18. Electrostatic potential energy was calculated to determine the interaction of these inhibitors with neighbouring residues of the protein. To assess the adopted simulation protocol, Area per lipid, membrane thickness, and EDP analysis were analysed. The backbone RMSD of Cα atoms were analysed to study the stability and convergence of membrane-bound α-Syn. To check the flexible and rigid regions of membrane-

bound α-Syn, RMSF were calculated from their corresponding trajectories obtained during MD simulation and plotted with respect to the residue index. The distance analysis between different regions of α-Syn in the absence and presence of α-Syn were plotted. The secondary structural analysis of α-Syn in the presence and absence of α-Syn were calculated using the Kabsch and Sander algorithm [295] and the percentage of secondary structure were calculated using YASARA software [258]. Intermolecular hydrogen bond analysis is used to analyse the proximity between the lipid bilayer and different regions of α-Syn in the absence and presence of inhibitors

4.4. Results and Discussions:

4.4.1. Area per Lipid analysis:

The surface area per lipid layer was calculated to determine the total surface area of the simulated box was divided by the total number of lipids in a single. By dividing the surface area of a biomembrane by the total amount of lipids in the system, one may determine its density. In the simulation system for DOPE/DOPS/DOPC, equilibrium configurations were determined by computing the average area per lipid surface (APL) as shown in **Figure 4.1**. The Area per lipid for the DOPE/DOPS/DOPC system was calculated for 67.78 $Å^2$ for the upper leaflet and 69.54 $Å^2$ for the lower leaflet over a 100 ns trajectory.

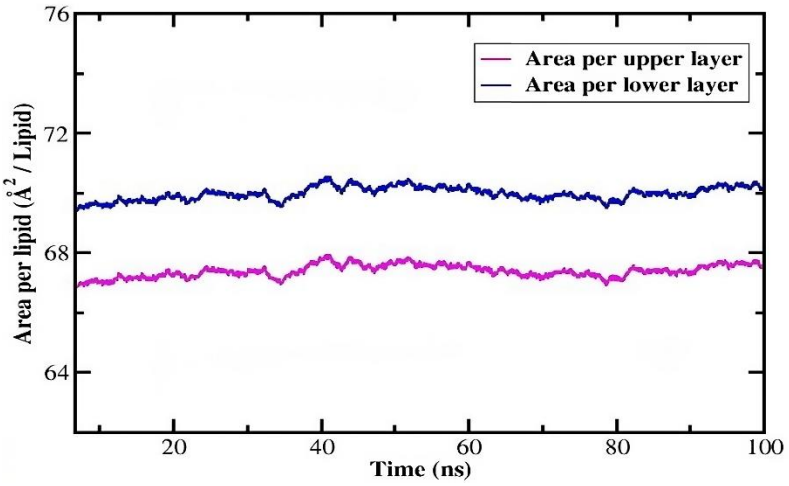

Figure 4.1. *Area per lipid analysis for α-Syn as a function of simulation time*

4.4.2. Membrane Thickness Analysis:

The membrane thickness plot **(Figure 4.2)** shows the time evolution of the membrane thickness for DOPE/DOPS/DOPC mixed lipid bilayers, which are stable for a simulated time of 100 ns. The shortest distance between each phosphorus atom in each leaflet of a lipid layer and every other phosphorus atom in the other leaflet of the lipid layer was used to calculate

the average membrane thickness. The average membrane thickness for the α-Syn was calculated to be 87.16 Å.

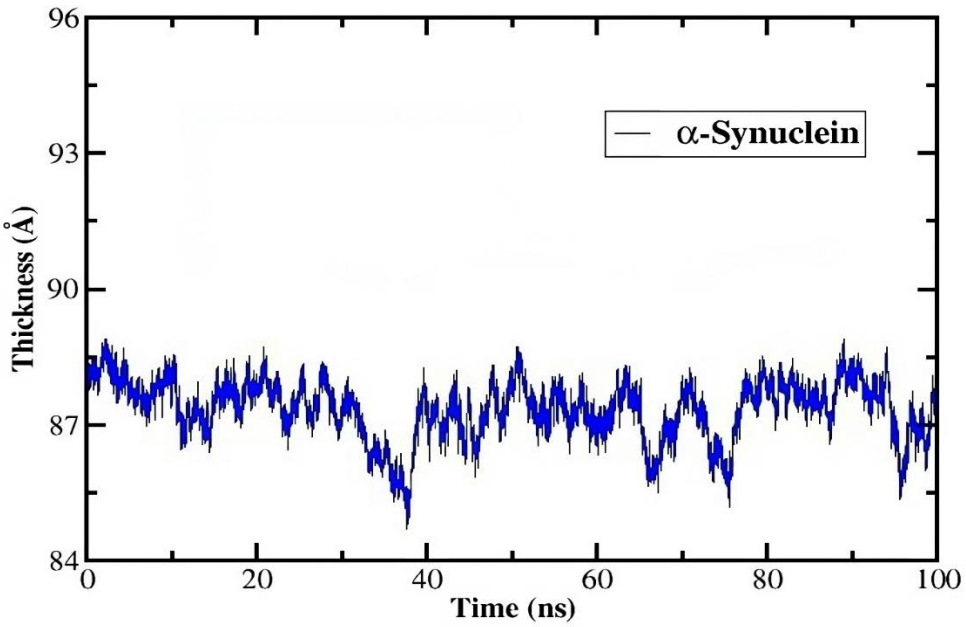

Figure 4.2. *Membrane thickness analysis for α-Syn as a function of simulation time*

4.4.3. Electron Density Profile Analysis:

The central electron charge of each atom was believed to be equal to the atomic number minus the atomic partial charge in order to calculate the electron density profile (EDP). Regarding all-atom densities, the density profiles of DOPE, DOPS, and DOPC exhibit three distinct zones. The mixed lipid bilayer is defined by the lipid bilayer made up of DOPE, DOPS, and DOPC formed in a 5:3:2 ratio on both lipid monolayers. EDP, as shown in **Figure 4.3**, are widely used to characterise the locations of molecules and their molecular constituents inside a lipid bilayer. The different regions of α-Syn is displayed in **Figure 4.4**. The N-helix region of both the α-Syn and complexes is discovered to be buried right below the lipid head group/water interface, enabling the protein's hydrophobic face to interact with the hydrophobic core of the lipid membrane and its hydrophilic face to connect with the polar region of the lipid and water. The N-helix of α-Syn tends to lie below the bilayer centre at a distance of 25 Å. In all the cases, Helix-N finishes up deeper than in the turn area, beneath the lipid head group phosphates.

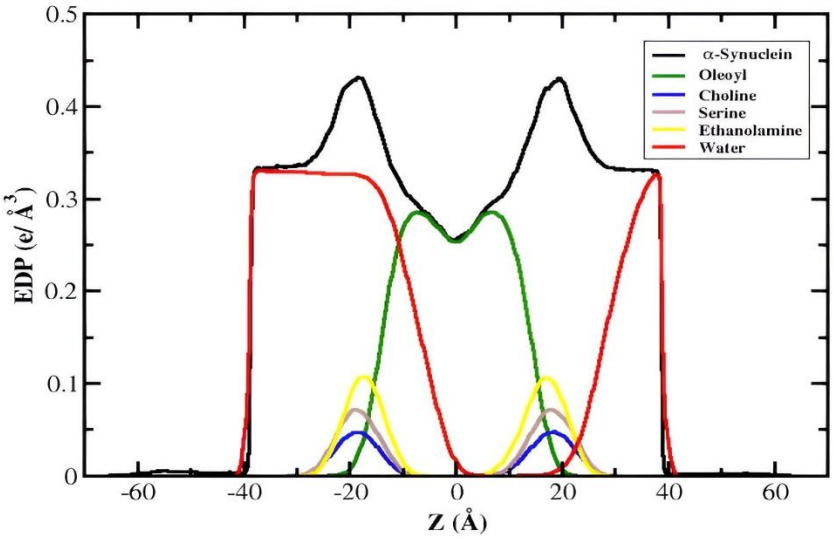

Figure 4.3. *Electron density profile analysis for α-Syn as a function of simulation time*

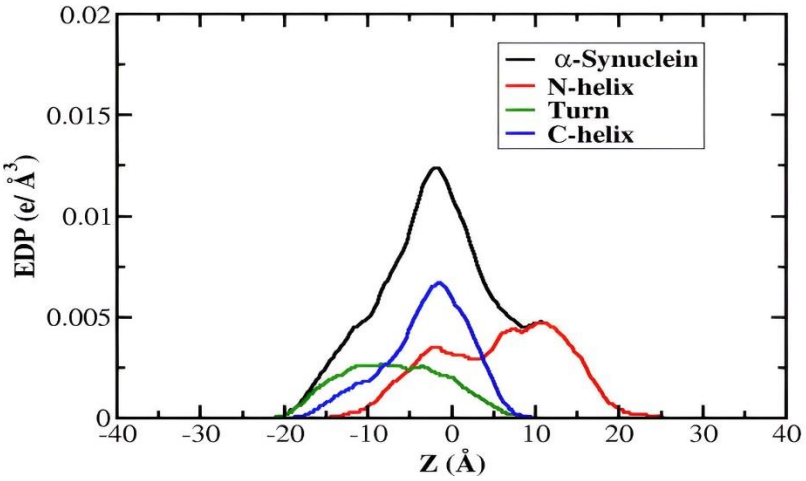

Figure 4.4. *Electron density profile analysis for each region of α-Syn as a function of simulation time*

4.4.4. Root mean square deviation Analysis:

In **Figure 4.5**, the RMSD analysis of the Cα atom for the α-Syn over the simulation period was determined. The overall structure of α-Syn was observed to adopt higher flexibility. In the case of **Figure 4.6**, the RMSD profile of each region of the α-Syn showed stable conformation in the N-terminal and C-terminal but the NAC region showed subtle changes in the conformation. The RMSD value was determined to be 10 Å.

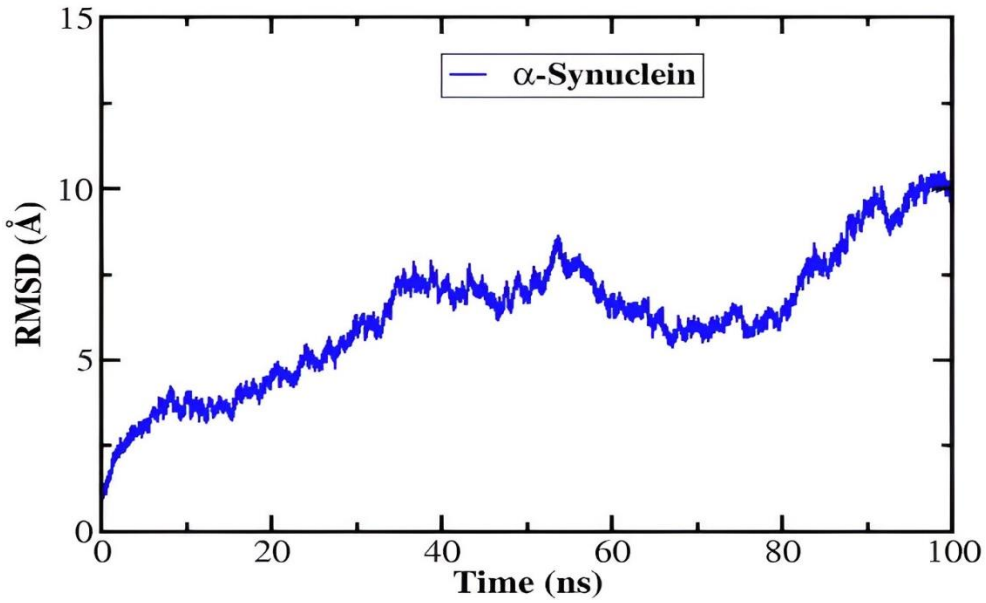

Figure 4.5. *RMSD analysis of α-Syn as a function of simulation time*

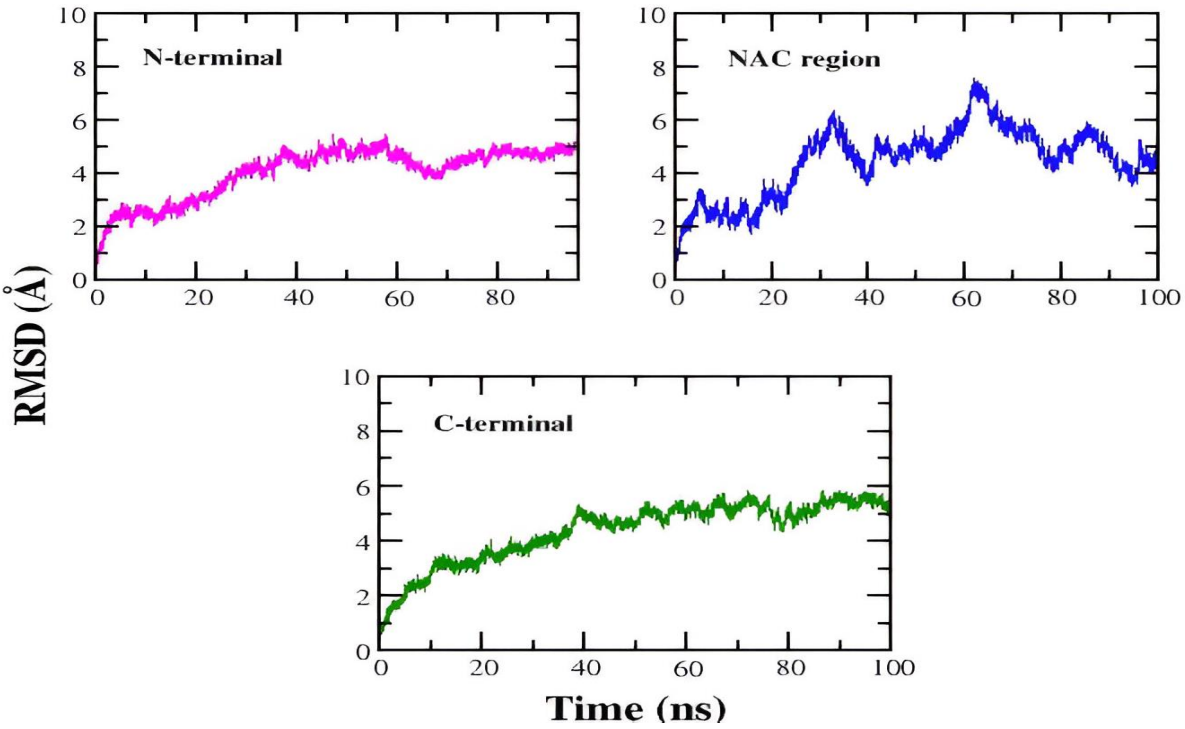

Figure 4.6. *RMSD analysis for each region of α-Syn as a function of simulation time*

4.4.5. Principle component analysis followed by Free Energy landscape analysis:

Free energy landscapes and PCA were employed to assess simulated α-Syn structures with and without inhibitors. The PCA was performed using the Cα atom's MD trajectory data, which was obtained after the systems had stabilised. In **Figure 4.7**, eigenvalues of α-Syn was shown to fluctuate more rapidly. It is noteworthy that a single global minimum and one or two

subsidiary minima were discovered for each system. On the other hand, it was discovered that the energy differential between secondary minima and global minima was at most 1.5 kcal/mol.

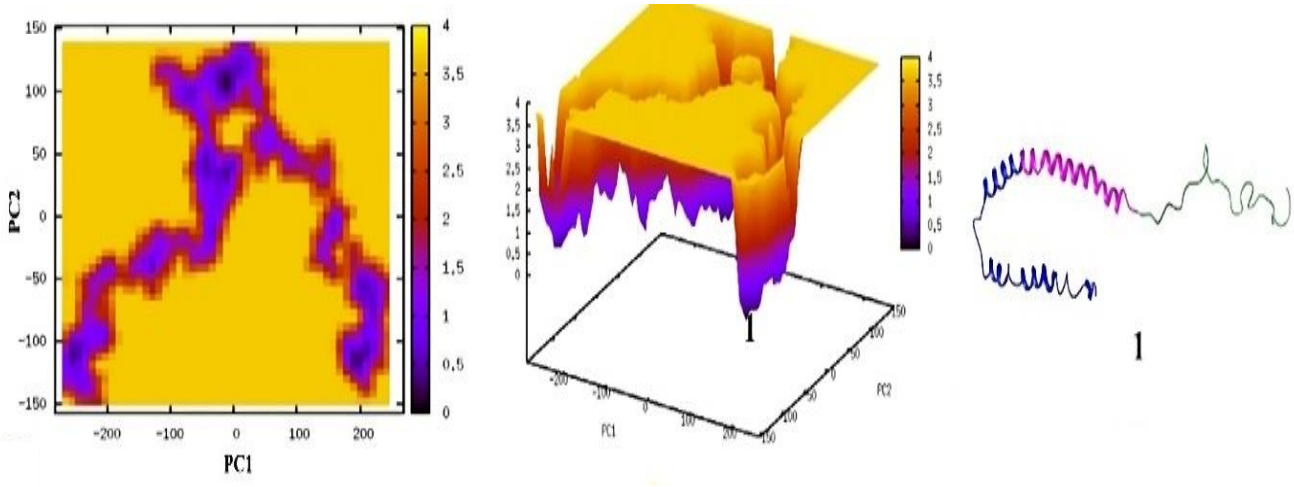

Figure 4.7. *PCA followed by 2D (left) and 3D (middle) free energy landscapes (FEL) analysis of α-Syn. X, Y, and Z indicate PC1, PC2, and free energy, respectively. In the energy well, '1', reflect the global minimum of α-Syn. Colour-coded mode was used to correlate structural conformations and free energy of α-Syn. The right-most panel shows energy wells with global free energy minima for α-Syn*

4.4.6. Root mean square fluctuation Analysis:

RMSF analysis with respect to the Cα atom has been performed in order to identify the flexible and rigid regions in the structure of α-Syn. The RMSF profile shown in **Figure 4.8** dictates relatively higher flexibility in α-Syn. The region near the NAC domain (40–70) of the α-Syn was observed to have higher flexibility.

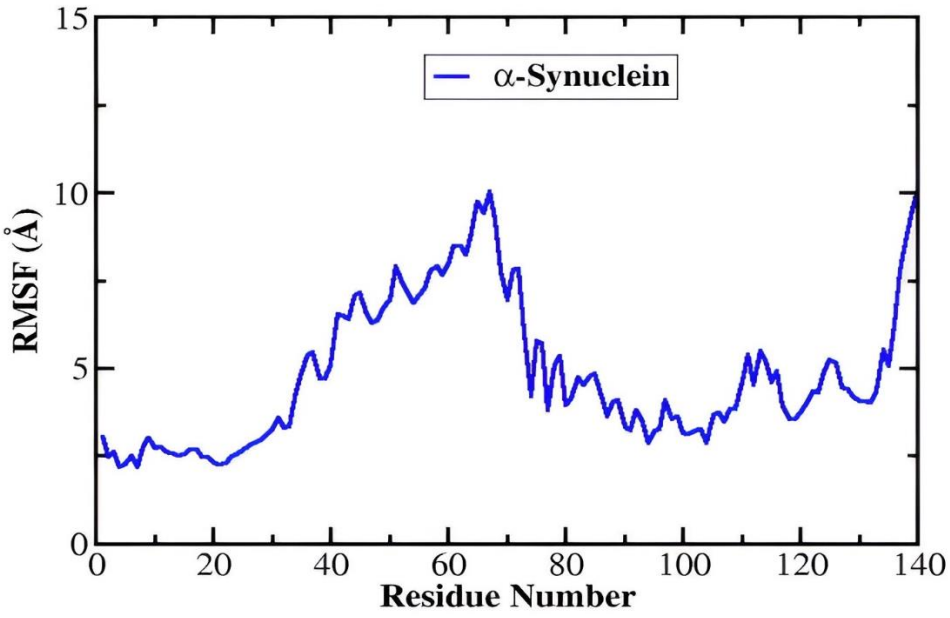

Figure 4.8. *RMSF analysis of α-Syn as a function of simulation time*

4.4.7. Secondary structural analysis:

Using the Kabsch and Sander method [295], the development of the secondary structure for the α-Syn was shown in **Figure 4.9**. The probable secondary structure was determined as observed in **Figure 4.10**. The percentage of secondary structure was calculated using YASARA software as tabulated in **Table 4.1**.

The percentage of α-helix, turn and coil region in α-Syn was calculated to be 18.9%, 25% and 53.6% respectively.

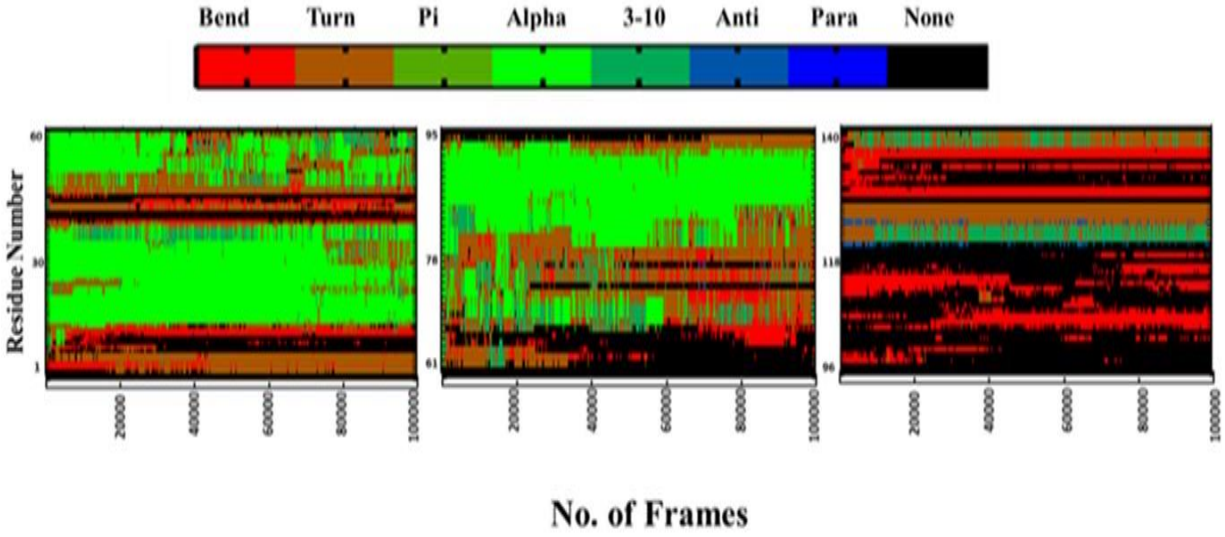

Figure 4.9. *DSSP plot of secondary Structural content of α-Syn during MD simulation obtained from Kabsch and Sander algorithm*

Table 4.1. *Secondary structural content of WT α-Syn during MD simulation*

COMPLEX	α-helix %	β-sheet %	turn %	Pi-helix %	3_{10} helix %	Coil %
α-Syn	18.9	1.1	25	0	1.4	53.6

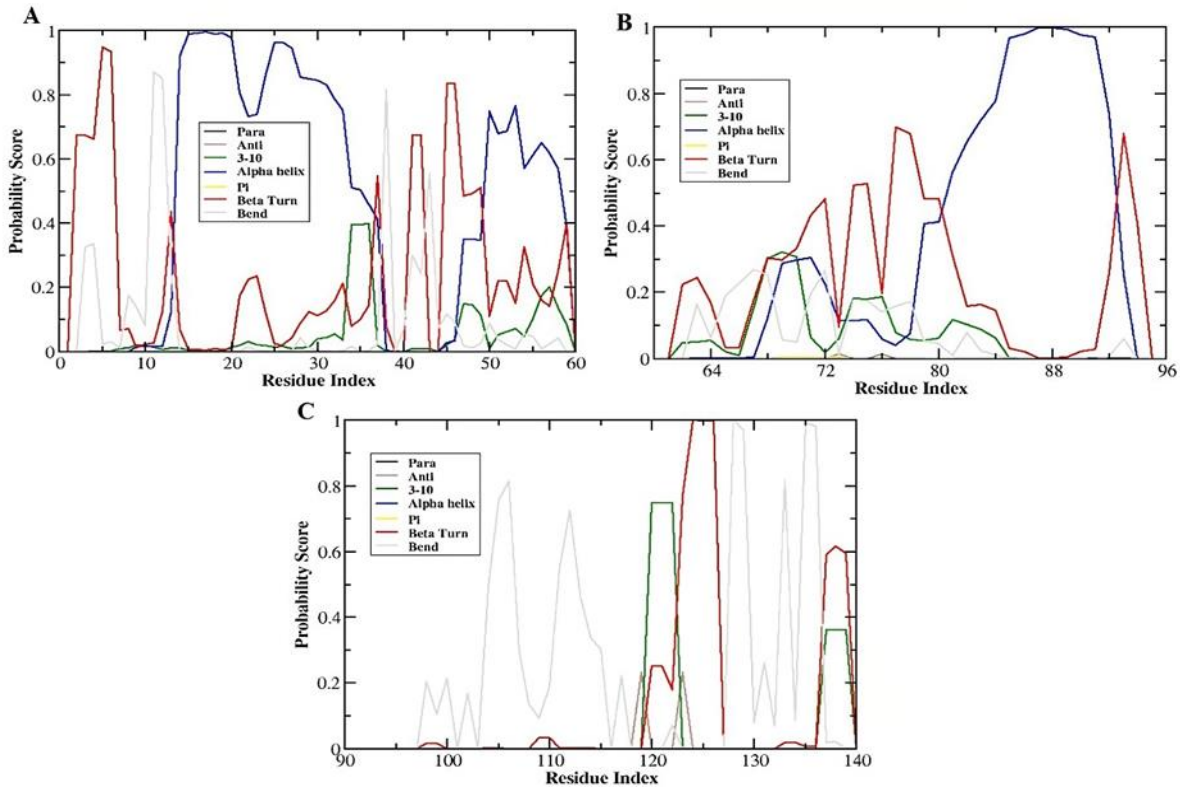

Figure 4.10. *Secondary structure Probability score of α-Syn during MD simulation*

4.4.8. Conformational snapshots of α-Synuclein in membrane bound state:

The snapshots of α-Syn was obtained from the MD simulation analysis as a function of time period. In **Figure 4.11**, the conformational dynamics of the α-Syn 3-D structure was depicted. The NAC region of α-Syn was observed to get elevated above the membrane surface and also observed the helix to be broken near the region 45–95. The α-helix can undergo an interconversion between two different conformations: an "extended helix," in which the regions (1-37) form a single helix that interacts with the lipid bilayer, and a "broken helix," in which the helix is broken at around the 45–95 position. In the bulk water phase, the α-Syn nucleus formed on the membrane attracts lipid-unbound monomers, which elongate to form long, unbranched amyloid fibrils along with a cross β-sheet structure.

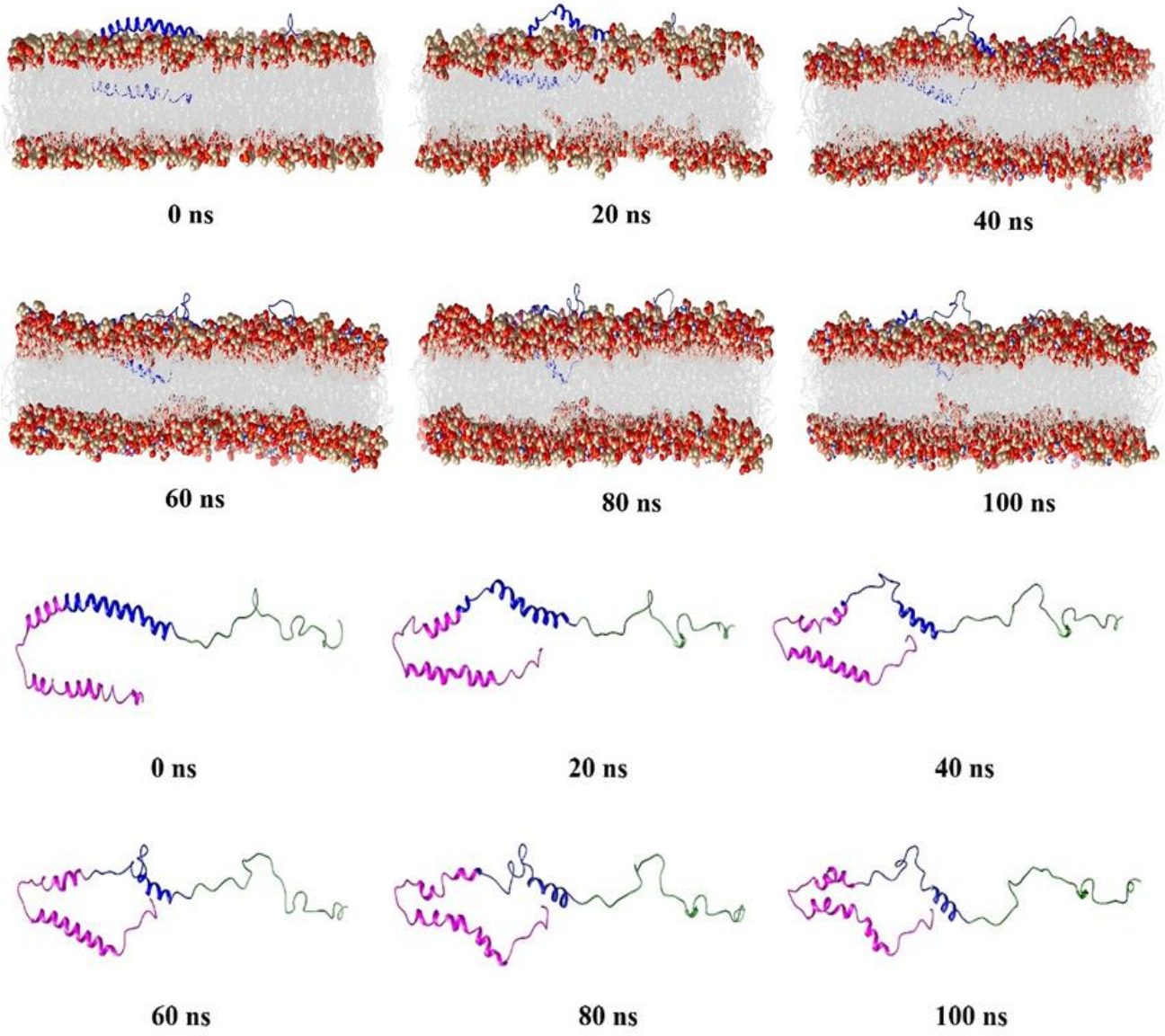

Figure 4.11.*Conformational snapshots of α-Syn during MD simulation*

4.4.9. Intermolecular Hydrogen bond analysis:

The intermolecular hydrogen bond analysis was performed as shown in **Figure 4.12** and **Figure 4.13** to examine the closeness between the lipid bilayer and various areas in the α-Syn. Among the three different regions of α-Syn, the NAC region of α-Syn was found to have a lesser number of hydrophobic contacts with the membrane. The atomic-level details regarding the intermolecular hydrogen bonds between the lipid bilayer (acceptor/donor) and α-Syn (acceptor/donor) were summarised in **Table 4.2** and **Table 4.3** respectively.

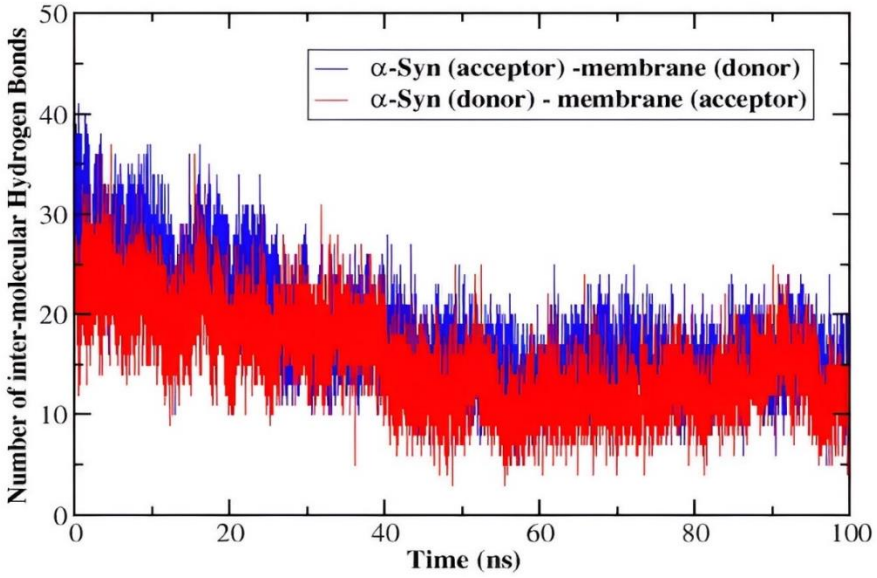

Figure 4.12. *Intermolecular hydrogen bond analysis of α-Syn during MD simulation*

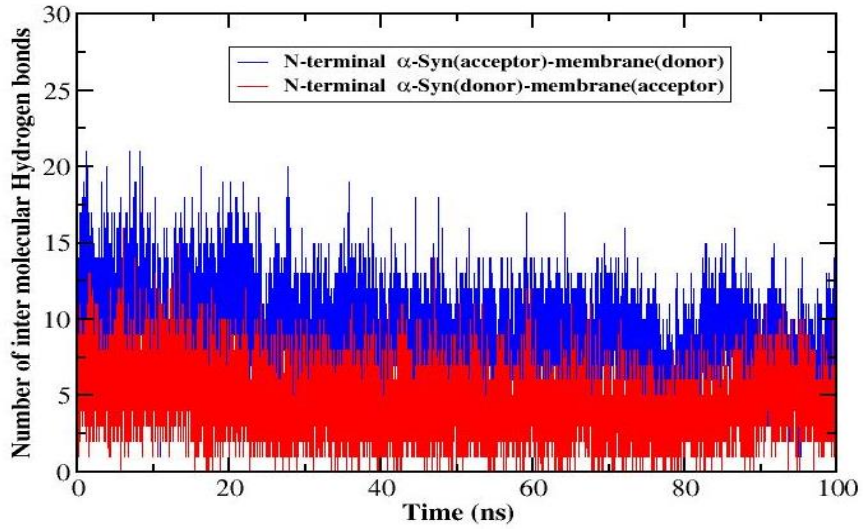

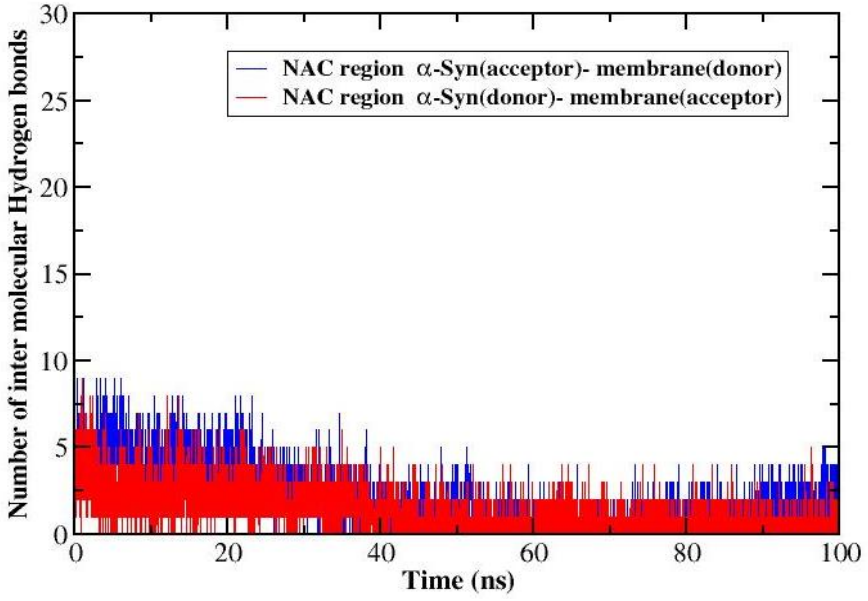

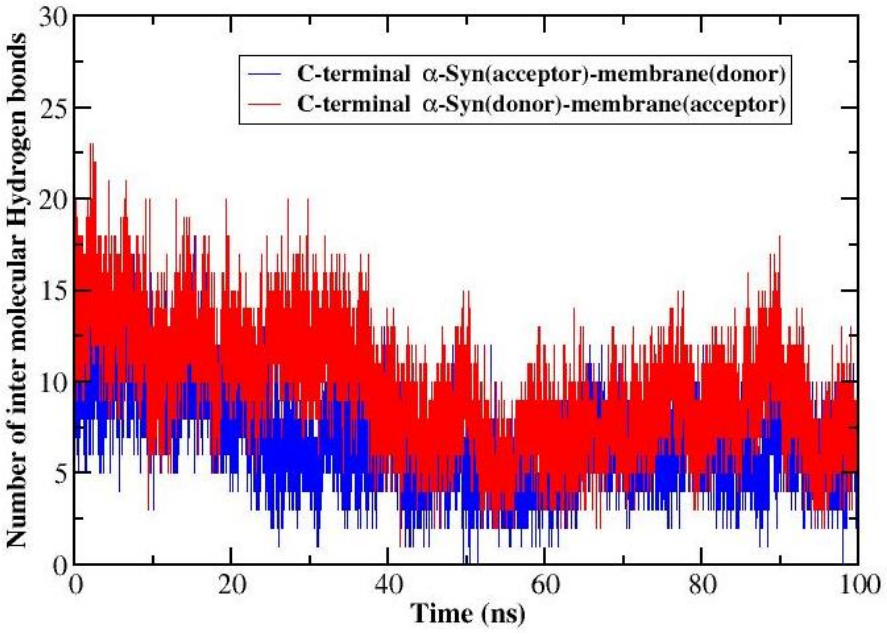

Figure 4.13. *Intermolecular hydrogen bond analysis of different regions of α-Syn during MD simulation*

Table 4.2. *Intermolecular Hydrogen bond analysis of membrane bound α-Syn complex during the MD simulation of 100 ns with membrane bilayer as acceptor and α-Syn as donor*

#Acceptor	DonorH	Donor	Average Distance (Å)	Average Angles (º)
PC_1771@O34	LYS_45@HZ2	LYS_45@NZ	2.7828	159.7695
PS_1801@O33	LYS_45@HZ1	LYS_45@NZ	2.755	158.4847
PC_1771@O34	LYS_45@HZ3	LYS_45@NZ	2.7837	158.6883
PC_1771@O22	LYS_45@HZ2	LYS_45@NZ	2.7611	157.456
PS_1837@O33	LYS_34@HZ1	LYS_34@NZ	2.7535	157.6146
PS_1804@O12	LYS_21@HZ3	LYS_21@NZ	2.7712	158.8013
PS_157@O35	LYS_12@HZ3	LYS_12@NZ	2.774	155.056
PE_151@O22	LYS_12@HZ1	LYS_12@NZ	2.7751	157.6401
PC_1771@O34	LYS_45@HZ1	LYS_45@NZ	2.786	158.509
PE_151@O22	LYS_12@HZ2	LYS_12@NZ	2.7725	157.1156
PS_1801@O33	LYS_45@HZ2	LYS_45@NZ	2.7512	158.504
PC_1771@O22	TYR_39@HH	TYR_39@OH	2.7036	163.6023
PC_1771@O22	LYS_45@HZ3	LYS_45@NZ	2.764	156.9784
PS_1804@O12	LYS_21@HZ1	LYS_21@NZ	2.7797	160.577
PE_1843@O33	LYS_6@HZ3	LYS_6@NZ	2.7431	159.1947
PE_1843@O33	LYS_6@HZ2	LYS_6@NZ	2.7402	157.7906
PS_157@O35	LYS_12@HZ2	LYS_12@NZ	2.7762	155.6836
PS_1801@O33	LYS_45@HZ3	LYS_45@NZ	2.7553	157.6606
PC_1771@O22	LYS_45@HZ1	LYS_45@NZ	2.7797	157.7347
PC_1828@O22	LYS_21@HZ2	LYS_21@NZ	2.7866	157.1097
PS_1804@O12	LYS_21@HZ2	LYS_21@NZ	2.7961	161.2667
PS_1801@O34	LYS_45@HZ1	LYS_45@NZ	2.7639	157.6868
PS_157@O35	LYS_12@HZ1	LYS_12@NZ	2.7638	155.6227
PS_157@O36	LYS_12@HZ3	LYS_12@NZ	2.7992	153.5915
PS_1804@O33	LYS_60@HZ2	LYS_60@NZ	2.739	159.0669
PS_1837@O34	LYS_34@HZ3	LYS_34@NZ	2.7562	154.5
PE_1843@O33	LYS_6@HZ1	LYS_6@NZ	2.756	157.252
PC_1828@O22	LYS_21@HZ3	LYS_21@NZ	2.8013	155.9808
PC_1828@O34	LYS_58@HZ3	LYS_58@NZ	2.741	156.5858
PS_1837@O33	LYS_34@HZ3	LYS_34@NZ	2.7672	157.4883

PS_1837@O22	LYS_34@HZ1	LYS_34@NZ	2.7547	153.4206
PS_1837@O36	LYS_43@HZ3	LYS_43@NZ	2.7623	151.9208
PS_1801@O34	LYS_45@HZ3	LYS_45@NZ	2.7618	157.3103
PS_1804@O36	LYS_60@HZ2	LYS_60@NZ	2.7685	155.6585
PE_1861@O22	GLY_41@H	GLY_41@N	2.8554	160.9231
PS_1837@O36	LYS_43@HZ1	LYS_43@NZ	2.7633	152.8834
PS_1837@O22	LYS_34@HZ3	LYS_34@NZ	2.7547	154.0497
PS_157@O36	LYS_12@HZ2	LYS_12@NZ	2.8151	152.7104
PE_151@O22	LYS_12@HZ3	LYS_12@NZ	2.773	156.6745
PS_1837@O22	LYS_34@HZ2	LYS_34@NZ	2.7626	153.5745
PE_1864@H2A	GLY_41@HA2	GLY_41@CA	2.8733	146.865
OL_143@H14S	LEU_8@H	LEU_8@N	2.7861	151.2152
PS_1837@O34	LYS_43@HZ3	LYS_43@NZ	2.7686	156.1343
PS_1804@O35	LYS_60@HZ2	LYS_60@NZ	2.7805	154.9642
PS_1804@O35	LYS_60@HZ1	LYS_60@NZ	2.7861	154.9721
PE_1834@O12	LYS_6@HZ3	LYS_6@NZ	2.7705	157.0186
PS_1804@O33	LYS_60@HZ1	LYS_60@NZ	2.7433	158.1793
PC_1828@O12	LYS_23@HZ3	LYS_23@NZ	2.7735	151.6139
PS_1837@O35	LYS_34@HZ1	LYS_34@NZ	2.7549	158.6713
PS_1804@O36	LYS_60@HZ1	LYS_60@NZ	2.795	155.642

Table 4.3. *Intermolecular Hydrogen bond analysis of membrane bound α-Syn complex during the MD simulation of 100 ns with membrane bilayer as donor and α-Syn as acceptor*

#Acceptor	DonorH	Donor	Average Distance (Å)	Average Angles (º)
LYS_43@O	PE_1864@HN1B	PE_1864@N31	2.799	152.0543
LYS_43@O	PE_1864@HN1C	PE_1864@N31	2.7858	153.0414
LYS_43@O	PE_1864@HN1A	PE_1864@N31	2.792	151.5234
GLU_57@OE1	PE_1825@HN1A	PE_1825@N31	2.7979	155.6097
GLY_41@HA2	PE_1864@H2A	PE_1864@C32	2.8727	147.6719
GLU_57@OE1	PE_1825@HN1B	PE_1825@N31	2.7824	153.5556
GLY_41@O	PE_1864@HN1C	PE_1864@N31	2.802	152.046
GLY_41@O	PE_1864@HN1B	PE_1864@N31	2.8102	151.0691
GLY_41@O	PE_1864@HN1A	PE_1864@N31	2.8148	151.3919
GLU_57@OE2	PE_1825@HN1B	PE_1825@N31	2.8064	154.1955
GLU_57@OE1	PS_1804@HN1A	PS_1804@N31	2.7925	159.3541
THR_54@OG1	PE_1855@HN1C	PE_1855@N31	2.8257	151.0641
GLU_57@OE1	PE_1825@HN1C	PE_1825@N31	2.7879	153.9006
THR_54@OG1	PE_1855@HN1B	PE_1855@N31	2.848	148.5822
LYS_6@HZ2	OL_1835@H8S	OL_1835@C18	2.8298	145.0043
LEU_8@H	OL_143@H14S	OL_143@C114	2.8002	148.6701
THR_54@OG1	PE_1855@HN1A	PE_1855@N31	2.8341	147.9113
LYS_32@HE2	OL_1854@H7S	OL_1854@C17	2.8756	145.7288
GLU_57@OE2	PE_1825@HN1C	PE_1825@N31	2.819	157.4003
GLY_51@O	PE_1855@HN1A	PE_1855@N31	2.8437	150.9603
LYS_34@HE3	PS_1837@HX	PS_1837@C2	2.8978	147.6915
GLY_14@HA3	OL_1818@H9R	OL_1818@C19	2.8773	145.5699
GLU_57@OE2	PE_1825@HN1A	PE_1825@N31	2.8141	156.9366
LYS_21@HE2	OL_1829@H3S	OL_1829@C13	2.8983	148.4765
GLU_57@OE1	PS_1804@HN1B	PS_1804@N31	2.811	161.3614
LEU_8@H	OL_143@H16S	OL_143@C116	2.8145	148.0205
LEU_8@H	OL_143@H15S	OL_143@C115	2.7765	148.5511
LEU_8@H	OL_143@H14R	OL_143@C114	2.8067	149.0427
LEU_8@H	OL_143@H16R	OL_143@C116	2.8148	149.1929
LYS_12@HE2	OL_152@H7S	OL_152@C17	2.8936	151.4801

LEU_8@H	OL_143@H15R	OL_143@C115	2.8081	149.1101
LYS_21@HE3	OL_1805@H3R	OL_1805@C13	2.8805	150.0826
GLY_14@HA2	OL_1820@H14R	OL_1820@C114	2.936	146.0151
GLY_51@O	PE_1855@HN1C	PE_1855@N31	2.8198	153.6304
ALA_53@O	PE_1825@HN1C	PE_1825@N31	2.8276	149.0664
ALA_17@HA	OL_1890@H10R	OL_1890@C110	2.8944	147.8631
LYS_21@HA	OL_1829@H9R	OL_1829@C19	2.9027	146.3457
LYS_21@HE3	OL_1805@H3S	OL_1805@C13	2.8767	147.2759
GLU_28@HA	OL_1854@H8R	OL_1854@C18	2.9321	144.64
MET_1@HB3	OL_1889@H9R	OL_1889@C19	2.8856	146.4726
GLN_24@HE22	OL_1829@H2R	OL_1829@C12	2.873	149.0738
MET_5@HG3	PE_1930@H2B	PE_1930@C32	2.9033	147.8884
TYR_39@H	OL_1860@H7R	OL_1860@C17	2.8771	156.7194
TYR_39@OH	PE_1864@HN1C	PE_1864@N31	2.8822	149.1039
LEU_8@H	OL_143@H12S	OL_143@C112	2.8514	150.8423
LYS_32@HB2	OL_1824@H9R	OL_1824@C19	2.9132	146.9812
LYS_12@HE2	OL_152@H7R	OL_152@C17	2.9038	152.3122
LYS_6@HZ3	OL_1835@H8S	OL_1835@C18	2.8698	143.8272
SER_9@H	OL_1844@H5S	OL_1844@C15	2.8641	155.3005
ALA_56@HB2	PS_1804@H2A	PS_1804@C32	2.9037	146.7501
LYS_32@HE2	OL_1854@H5S	OL_1854@C15	2.8738	144.7549
LYS_21@HE3	OL_1805@H2R	OL_1805@C12	2.8741	145.6414

4.4.10. Distance analysis:

The centre of mass distance between the various α-Syn domains has been measured as depicted in **Figure 4.14**. The centre of mass distance between the various α-Syn regions was found to decreasing than the distance between the NAC and C terminal area. An increase in the distance between the NAC area and C-terminal centre of mass corresponds with the degree to which α-Syn was raised, resulting in bending of the NAC region that finally changed its structural conformation.

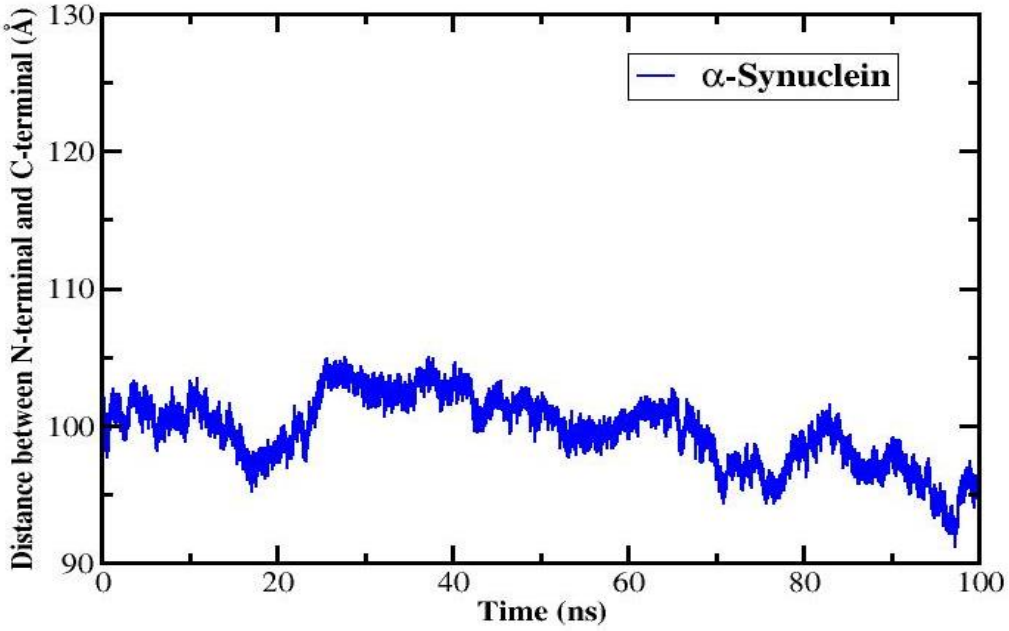

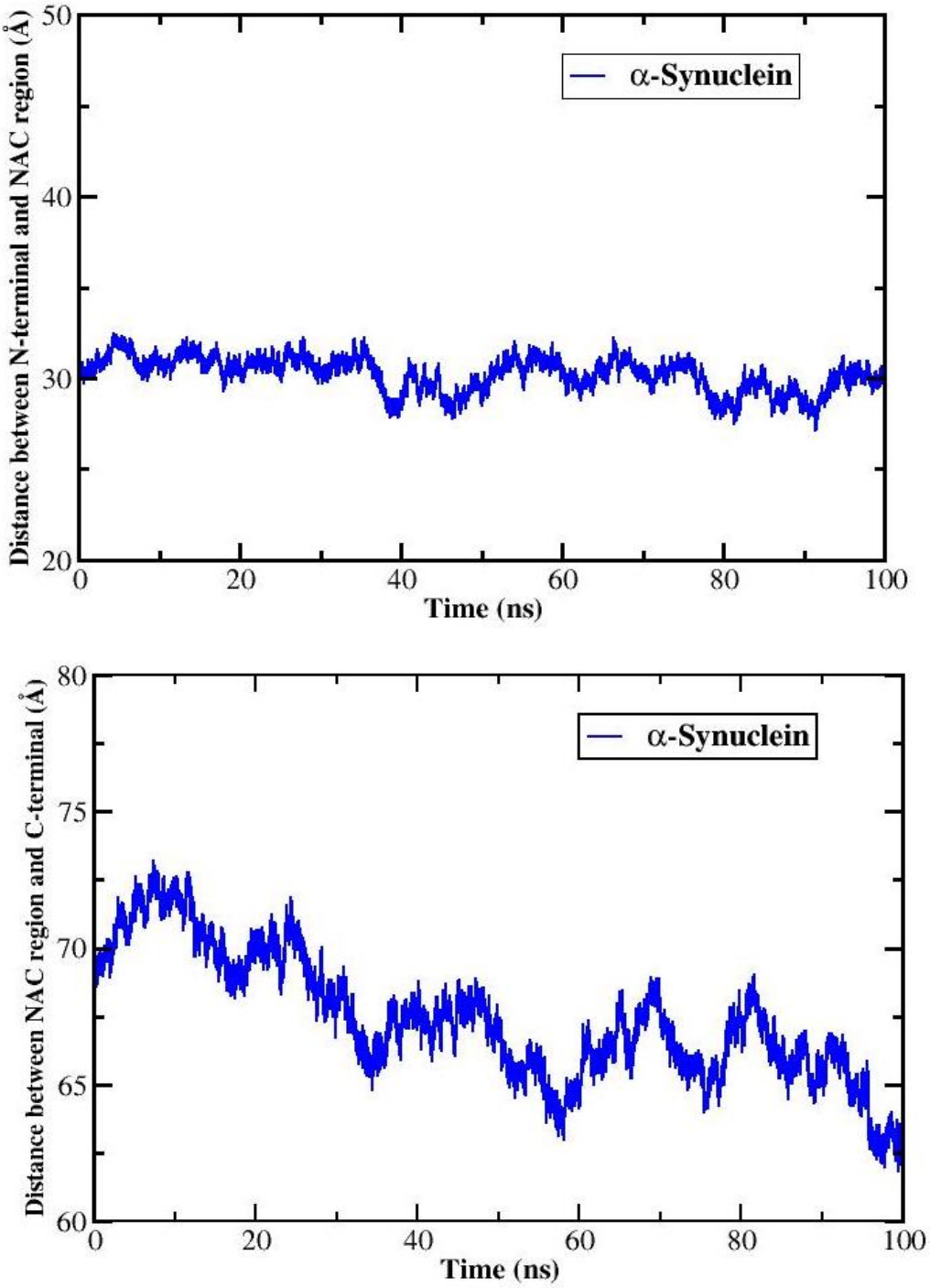

Figure 4.14. *Distance analysis of α-Syn during MD simulation as a function of simulation time*

4.5. Conclusion:

In general, it is noted that the penetration of α-Syn into the membrane rapidly influences its transition from α-helical to a coiled structure. This penetration also aids in the incorporation of additional free α-Syn monomers into the complex, which causes phospholipids to displace and oligomers to form in the membrane. In our study, α-Syn adopts well-defined α-helical structures

during its interaction with lipid membranes, which inhibits the transition of the α-helical secondary structure into a coiled structure. And also, the NAC region of α-Syn was observed to expose itself from the lipid bilayer surface, which plays a role in the interconversion between the "extended" and "broken-helix" states and consequently leads to the formation of conformational intermediates that are prone to aggregation.